THE JOURNAL OF PHYSICAL CHEMISTRY A

Article

pubs.acs.org/JPCA

Two-Photon Absorption in Conjugated Energetic Molecules

Josiah A. Bjorgaard,[‡,§] Andrew E. Sifain,[∥] Tammie Nelson,[§] Thomas W. Myers,[⊥] Jacqueline M. Veauthier,[⊥] David E. Chavez,[⊥] R. Jason Scharff,[*,#] and Sergei Tretiak[*,▽,‡,§]

[‡]Center for Nonlinear Studies, [§]Theoretical Division, Physics and Chemistry of Materials (T-1), [⊥]Chemistry Division, [#]Explosives Science and Shock Physics Division, Shock and Detonation Physics (M-9), and [▽]Center for Integrated Nanotechnologies, Los Alamos National Laboratory, Los Alamos, New Mexico 87545, United States

[∥]Department of Physics and Astronomy, University of Southern California, Los Angeles, California 90089-0484, United States

Supporting Information

ABSTRACT: Time-dependent density functional theory (TD-DFT) was used to investigate the relationship between molecular structure and the one- and two-photon absorption (OPA and TPA, respectively) properties of novel and recently synthesized conjugated energetic molecules (CEMs). The molecular structures of CEMs can be strategically altered to influence the heat of formation and oxygen balance, two factors that can contribute to the sensitivity and strength of an explosive material. OPA and TPA are sensitive to changes in molecular structure as well, influencing the optical range of excitation. We found calculated vertical excitation energies to be in good agreement with experiment for most molecules. Peak TPA intensities were found to be significant and on the order of 10^2 GM. Natural transition orbitals for essential electronic states defining TPA peaks of relatively large intensity were used to examine the character of relevant transitions. Modification of molecular substituents, such as additional oxygen or other functional groups, produces significant changes in electronic structure, OPA, and TPA and improves oxygen balance. The results show that certain molecules are apt to undergo nonlinear absorption, opening the possibility for controlled, direct optical initiation of CEMs through photochemical pathways.

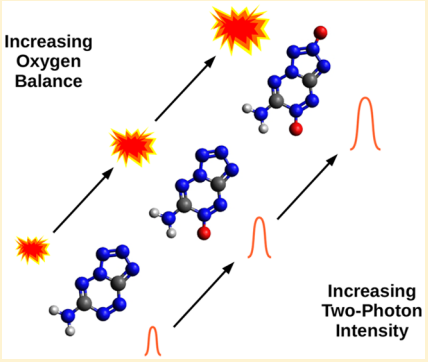

INTRODUCTION

There has been an increasing effort to understand the factors influencing two-photon absorption (TPA). Investigations have included a wide variety of molecular structures ranging from dipolar and quadrupolar structures[1−10] to multimeric complex structures.[11−21] Conjugated energetic molecules (CEMs) are a recently developed class of materials combining the optical properties of carbon-based conjugated organic molecules with the high nitrogen content typically found in high explosives (HEs). Recent publications have detailed the synthesis of various CEMs.[22−27] The large numbers of C−N and N−N bonds in CEMs increases their heats of formation compared to those of conventional carbon-based conjugated molecules, thus making them energetic.[28] The resulting high heats of formation and strong light-absorbing properties make CEMs promising candidates for applications in the direct optical initiation of photoactive HEs.[29] Measuring the nonlinear optical properties of HEs is difficult, however, because of practical considerations. Herein, we report a study of the optical properties of these molecules with variations in their chemical structure to find design principles for further developments.

Most HEs are nitramines, which absorb in the ultraviolet range, making it difficult to develop stable HEs that can be resonantly excited using standard lasers. The conventional optical initiation mechanisms require high laser intensities and proceed through indirect mechanisms such as thermal or shock processes.[30−32] On the other hand, CEMs can have cross sections for both one-photon absorption (OPA) and TPA in optical ranges so that these processes can be excited by conventional lasers. Excitation of these active electronic states could lead to decomposition through a photochemical pathway. This process is herein termed direct optical initiation.[29,33] TPA response is of particular interest for the direct optical initiation mechanism because it provides a means to select the low frequency range and intensity of light to ignite the explosive. TPA properties of conjugated high-N molecules, however, have not been examined to date.

It is well-known that molecular structure influences the TPA response of carbon-based conjugated organic materials.[1,2,4] Molecular structure is also essential in determining the overall performance of an HE. Functionalization of a core framework is often used to achieve the desired oxygen balance and improve the heat of formation, influencing the sensitivity and strength of the HE.[28] In this study, we seek to determine structure−property relationships of CEMs using time-dependent density functional theory (TD-DFT)[34] to understand the effects that variations in molecular structure have on OPA and TPA,[35] particularly with the addition of functional groups such as NO_2,

Received: March 27, 2016
Revised: June 2, 2016
Published: June 3, 2016

DOI: 10.1021/acs.jpca.6b03136
J. Phys. Chem. A 2016, 120, 4455−4464

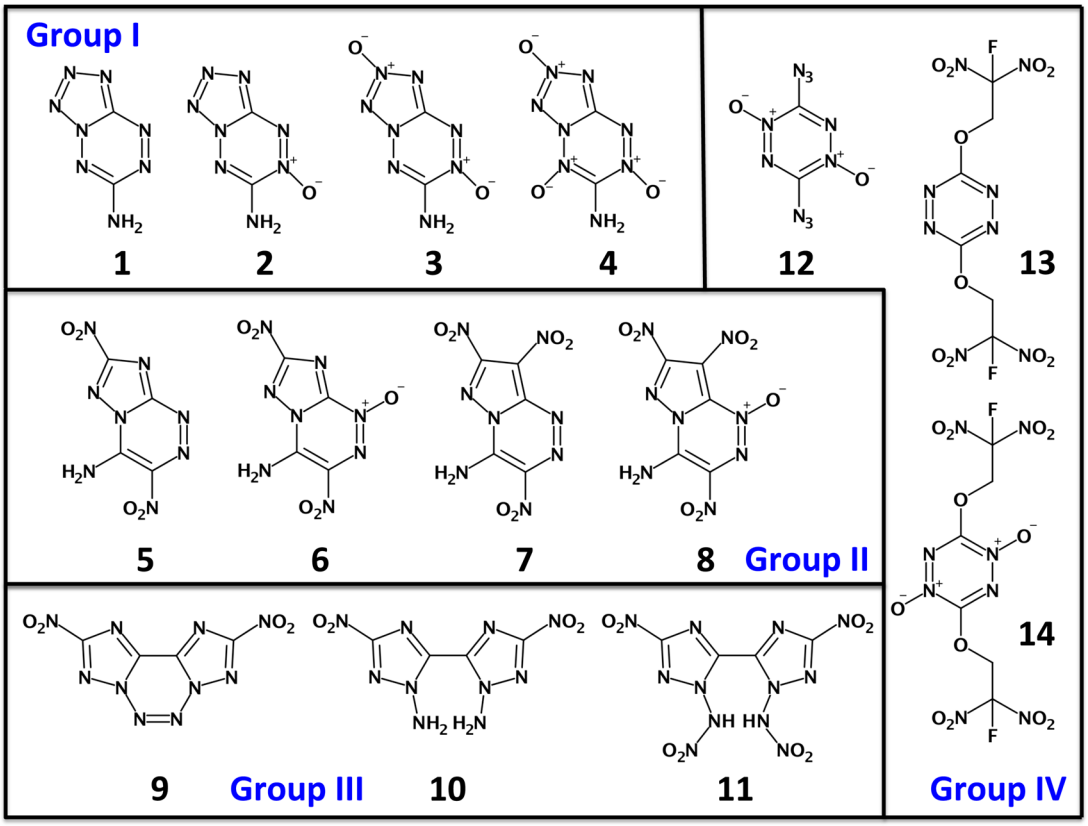

Figure 1. Chemical structures of conjugated energetic molecules.

NH_2, and O typically used to fine-tune the oxygen balance and heat of formation. This could lead to a tailored-design for future energetic materials with desired TPA responses.

METHODS

Theoretical predictions of TPA cross sections can be obtained using the extension of adiabatic TD-DFT to nonlinear optical response calculations.[35] TD-DFT offers a resonably accurate and computationally feasible method for calculating the optical responses and excited-state electronic structures of large molecular systems.[36,37] In this work, we used TD-DFT to calculate the OPA and TPA cross sections of the CEMs shown in Figure 1.

To obtain theoretical predictions for the one- and two-photon cross sections, optimized ground-state geometries were computed using Hartree−Fock (HF) theory and a 6-31+G* basis,[38] whereas vertical excitation energies were computed using TD-DFT and the B3LYP functional[39] with a 6-31G(d′) basis. Although it has been reported that HF geometries are less accurate than DFT geometries when compared to experimental data, the HF and TD-B3LYP combination has produced qualitatively accurate linear and nonlinear optical spectra over a wide range of molecular sizes for conjugated organic materials.[3,14,40] All quantum-chemical calculations were done in the Gaussian 03 and 09 software packages.[41,42] TPA cross sections were calculated from the TD-DFT results following ref 35. These calculations require a broadening parameter for a Lorentzian line shape, which we choose to be 0.06 eV; a reasonable value at room temperature for this family of chromophores.

Natural transition orbital (NTO) analysis of the electronic transitions dominating TPA was performed. NTOs offer the most compact, qualitative representation of a specified transition density expanded in terms of single-particle transitions.[43] Therefore, NTOs provide a useful way to assign the transition character as either $\pi-\pi^*$, charge transfer (CT), or a mixture of the two. Figures showing optimized molecular geometries and NTOs were obtained with the Avogadro program.[44]

Oxygen balance (OB%) provides a measure of the degree to which a material can be oxidized. In the case of HEs, we have defined it as the percentage of oxygen required for complete oxidation of carbon, hydrogen, and metal to form their respective oxides. The CEMs analyzed in this work do not contain metal atoms, allowing the oxygen balance to be computed as

$$\mathrm{OB\%} = -1600\left(2X + \frac{1}{2}Y - Z\right)/M \tag{1}$$

where X, Y, and Z refer to the number of carbon, hydrogen, and oxygen atoms, respectively, and M is the molecular weight of the compound. The optimal performance is generally achieved as OB% approaches zero.

Experimental extinction coefficients ϵ^{M} (M indicates measured) were determined from absorption spectra recorded with an HP 8453 Agilent UV−vis spectrometer. Materials were dissolved in solutions of acetonitrile at concentrations on the order of 10^{-4} M. The extinction coefficient was determined from the average of three solutions. A calculated extinction coefficient ϵ was determined from the results of TD-DFT calculations using the equation

DOI: 10.1021/acs.jpca.6b03136
J. Phys. Chem. A 2016, 120, 4455−4464

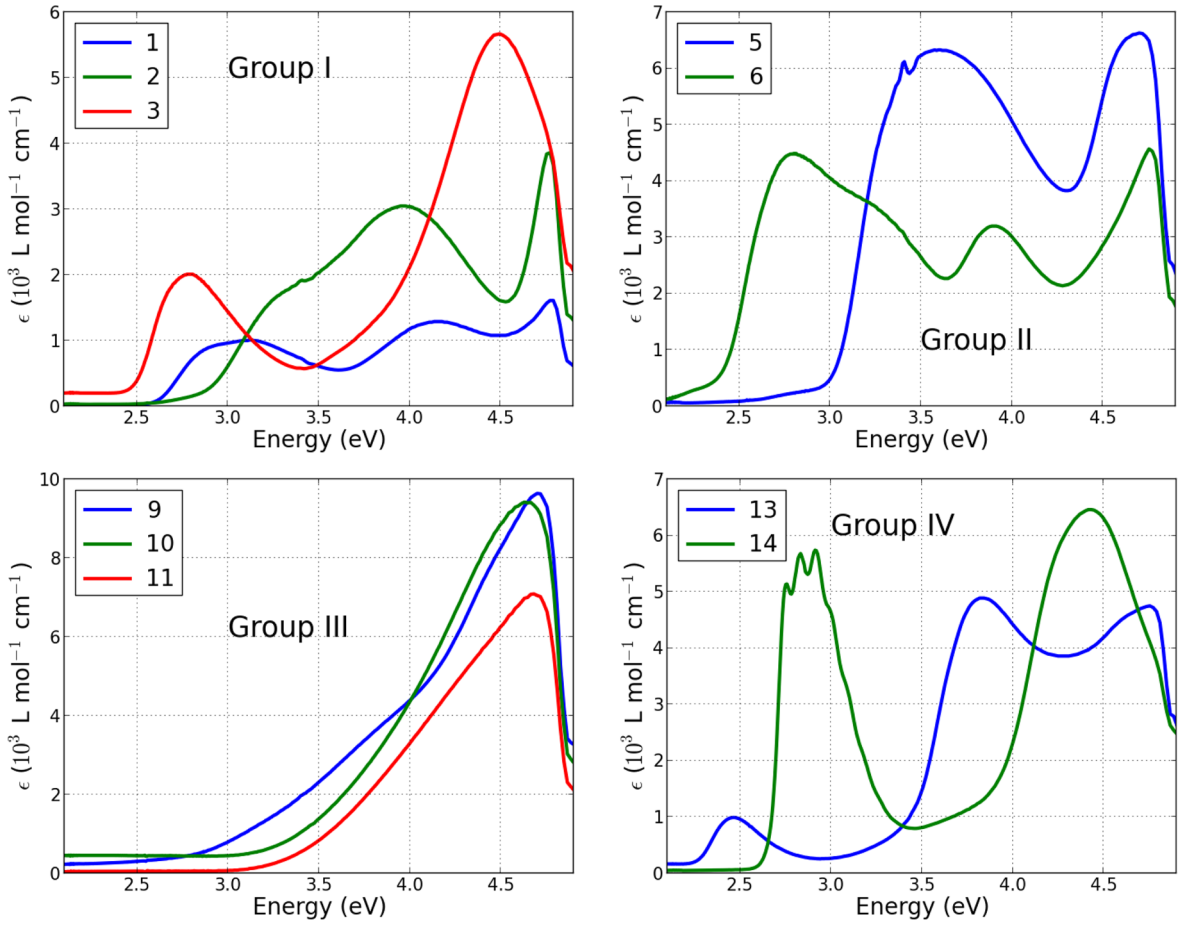

Figure 2. Experimental extinction coefficients determined in acetonitrile for groups I–IV of the molecules given in Figure 1.

$$\epsilon(\Omega) = \frac{e^2 N_A h}{9.212\epsilon_0 m_e c\sqrt{2\pi\gamma^2}} f_{0i} \exp[-(\Omega - \Omega_{0i})^2/2\gamma^2] \quad (2)$$

where Ω is photon energy; e is the electron charge; N_A is Avogadro's number; h is Planck's constant; ϵ_0 is the dielectric permittivity of vacuum; γ is a broadening parameter chosen here to be 0.1 eV; and f_{0i} and Ω_{0i} are the oscillator strength and transition energy, respectively, for the transition from the ground state to state i.

RESULTS

Calculated maximum OPA energies and extinction coefficients were compared to experimental values from spectra given in Figure 2. Data for calculated OPA and TPA and experimental extinction coefficients are summarized in Table 1. Whereas experiments were performed in solutions of acetonitrile, all simulations were performed in the gas phase. This can give a disagreement of up to 0.5 eV in transition energies, being mostly systematically red-shifted, and can affect the calculated extinction coefficients.[45] For all molecules with experimental data, we found that the relative vertical excitation energies and extinction coefficients were in good agreement. This gives us confidence in the accuracy of our calculated TPA results, for which no experimental data exist. Previous studies have shown that TPA cross sections simulated by this method provide results comparable to experiment.[3] Notably, for simulations of TPA spectra, only the relative energies are of importance.[35]

The molecules were categorized into four groups (Figure 1). Group I includes molecules **1**–**4**;[22,23] group II, **5**–**8**; group III, **9**–**11**;[24] and group IV, **12**–**14**.[25−27] Results of simulated spectra were compared across all groups and then within the framework of variations in chemical structure. We note here that we discuss only TPA frequencies below the first one-photon transition energy. One-photon resonances and excited-state absorptions do not allow for the evaluation of TPA overlapping with linear absorption spectra. Thus, TPA peaks that shift above this frequency after changing chemical structure might be absent and are therefore not discussed.

Group I. Group I consists of molecules with a bicyclic framework that vary in the number of O substituents and, therefore, in oxygen balance. Optical spectra are given in Figure 3. The simulated OPA of **1** has three peaks, approximately evenly spaced, the lowest of which is centered at 2.7 eV. A single O substituent raises the OPA energies in **2**, whereas two and three O substituents produce a peak at ∼3 eV in **3** and **4**, respectively. The positions and magnitudes of the higher-energy peaks vary with different numbers of O substituents.

The TPA intensity of **1** is small, although a larger, higher-energy peak cannot be ruled out because it might be outside of the spectral window. NTO analysis (Table S1 in the Supporting Information) shows two-photon-active excitations of **1** and **2** having predominantly π–π^* character. A high-energy peak occurs in **2** at 110 GM. The low-energy TPA peak corresponding to the lowest OPA peak is absent in **1** and is very small in **2**, but occurs in **3** at 20 GM. This peak decreases to 7 GM in **4**. A high-energy peak occurs in **3** with a magnitude

DOI: 10.1021/acs.jpca.6b03136
J. Phys. Chem. A 2016, 120, 4455−4464

Table 1. Summary of Calculated and Measured (M) Results for One-Photon and Two-Photon Absorption Cross Sections[a]

μ_{gg} (D)	Ω_{OPA} (eV)	ϵ_{max} (L mol^{-1} cm^{-1})	Ω^{M}_{OPA} (eV)	ϵ^{M}_{max} (L mol^{-1} cm^{-1})	Ω_{TPA} (eV)	σ_2^{max} (GM)	type
				Molecule **1**			
6.31	2.72	1.5×10^3	3.13	1.0×10^3			
	3.75	9.8×10^3	4.18	1.3×10^3			
	4.74	2.4×10^4	4.79	1.6×10^3	4.74	2	$\pi-\pi^*$
				Molecule **2**			
7.17	4.02	1.0×10^4	3.98	3.1×10^3			
	4.41	4.7×10^4	4.77	3.9×10^3			
	5.80	2.3×10^4					
	6.42	2.7×10^5					
					6.76–6.78	110	$\pi-\pi^*$
				Molecule **3**			
7.88	3.00	4.2×10^4	2.81	2.0×10^3	3.00	20	$\pi-\pi^*$/CT
	4.40	6.6×10^3	4.50	5.7×10^3	4.40	20	$\pi-\pi^*$/CT
	4.77	8.6×10^4					
					4.93–4.97	110	$\pi-\pi^*$/CT
				Molecule **4**			
6.87	3.12	4.0×10^4			3.12	7	$\pi-\pi^*$/CT
	3.94	2.7×10^4			3.91–3.94	10	$\pi-\pi^*$/CT
	4.75	1.2×10^5			4.70–4.75	20	$\pi-\pi^*$
	5.29	6.7×10^4			5.28–5.32	9	$\pi-\pi^*$/CT
				Molecule **5**			
5.36	3.23	1.1×10^3	3.61	6.3×10^3			
	4.45	7.4×10^4	4.70	6.6×10^3	4.54–4.57	10	$\pi-\pi^*$/CT
	5.25	1.3×10^4			5.25	20	$\pi-\pi^*$/CT
					5.50–5.53	8	$\pi-\pi^*$/CT
	5.69	1.0×10^5			5.66–5.69	5	$\pi-\pi^*$/CT
					5.82–5.85	9	$\pi-\pi^*$/CT
	5.90	1.0×10^5					
				Molecule **6**			
4.93	3.15	4.8×10^4	2.81	4.5×10^3	3.15	10	$\pi-\pi^*$/CT
	3.67	3.5×10^4	3.91	3.2×10^3	3.67	9	$\pi-\pi^*$/CT
	4.42	3.6×10^4	4.75	4.6×10^3	4.42	20	$\pi-\pi^*$
	5.33	3.4×10^4					
				Molecule **7**			
6.50	4.13	1.6×10^5					
	4.51	2.8×10^4			4.48–4.51	40	$\pi-\pi^*$
					5.19–5.24	130	$\pi-\pi^*$/CT
	5.41	1.1×10^5			5.33–5.46	200	$\pi-\pi^*$/CT
				Molecule **8**			
5.74	3.08	4.8×10^4			3.08	9	$\pi-\pi^*$/CT
	3.68	6.0×10^4			3.68	30	$\pi-\pi^*$/CT
	4.30	3.4×10^4			4.26–4.30	70	$\pi-\pi^*$/CT
	4.86	2.1×10^4			4.86	60	$\pi-\pi^*$/CT
				Molecule **9**			
1.93	4.56	6.9×10^3	4.70	9.6×10^3			
	5.08	2.9×10^4					
	5.72	1.2×10^5			5.57–5.72	40	$\pi-\pi^*$/CT
				Molecule **10**			
4.23	5.45	7.5×10^4	4.63	9.4×10^3	5.47	20	$\pi-\pi^*$/CT
	6.00	1.5×10^5			5.98–6.02	17	$\pi-\pi^*$/CT
				Molecule **11**			
3.52	5.02	2.7×10^3	4.68	7.1×10^3			
					5.45–5.60	10	$\pi-\pi^*$/CT
	5.70	8.50×10^4					
				Molecule **12**			
2.75	3.01	6.4×10^4					
	3.97	5.0×10^4					
	4.88	3.1×10^4			4.90	191	$\pi-\pi^*$
					5.20	265	$\pi-\pi^*$
	5.49	1.9×10^5					

DOI: 10.1021/acs.jpca.6b03136
J. Phys. Chem. A 2016, 120, 4455–4464

Table 1. continued

μ_{gg} (D)	Ω_{OPA} (eV)	ϵ_{max} (L mol^{-1} cm^{-1})	Ω^{M}_{OPA} (eV)	ϵ^{M}_{max} (L mol^{-1} cm^{-1})	Ω_{TPA} (eV)	σ_2^{max} (GM)	type
			Molecule **13**				
4.00	2.23	1.8×10^3	2.47	9.9×10^2			
					3.82	2	CT
	4.30	1.5×10^4	3.84	4.9×10^3			
			Molecule **14**				
4.94	3.00	5.9×10^3	2.91	5.7×10^3	3.00	2	CT/π–π*
					3.24	2	CT/π–π*
	3.45	4.7×10^4			3.54	2	CT

[a]Ground-state dipole moments μ_{gg}, absorption energies Ω_{OPA}, extinction coefficients ϵ_{max}, TPA energies Ω_{TPA}, maximum TPA cross sections σ_2^{max}, and qualitative characterization of the one-photon- and two-photon-active excited states based on NTO analysis.

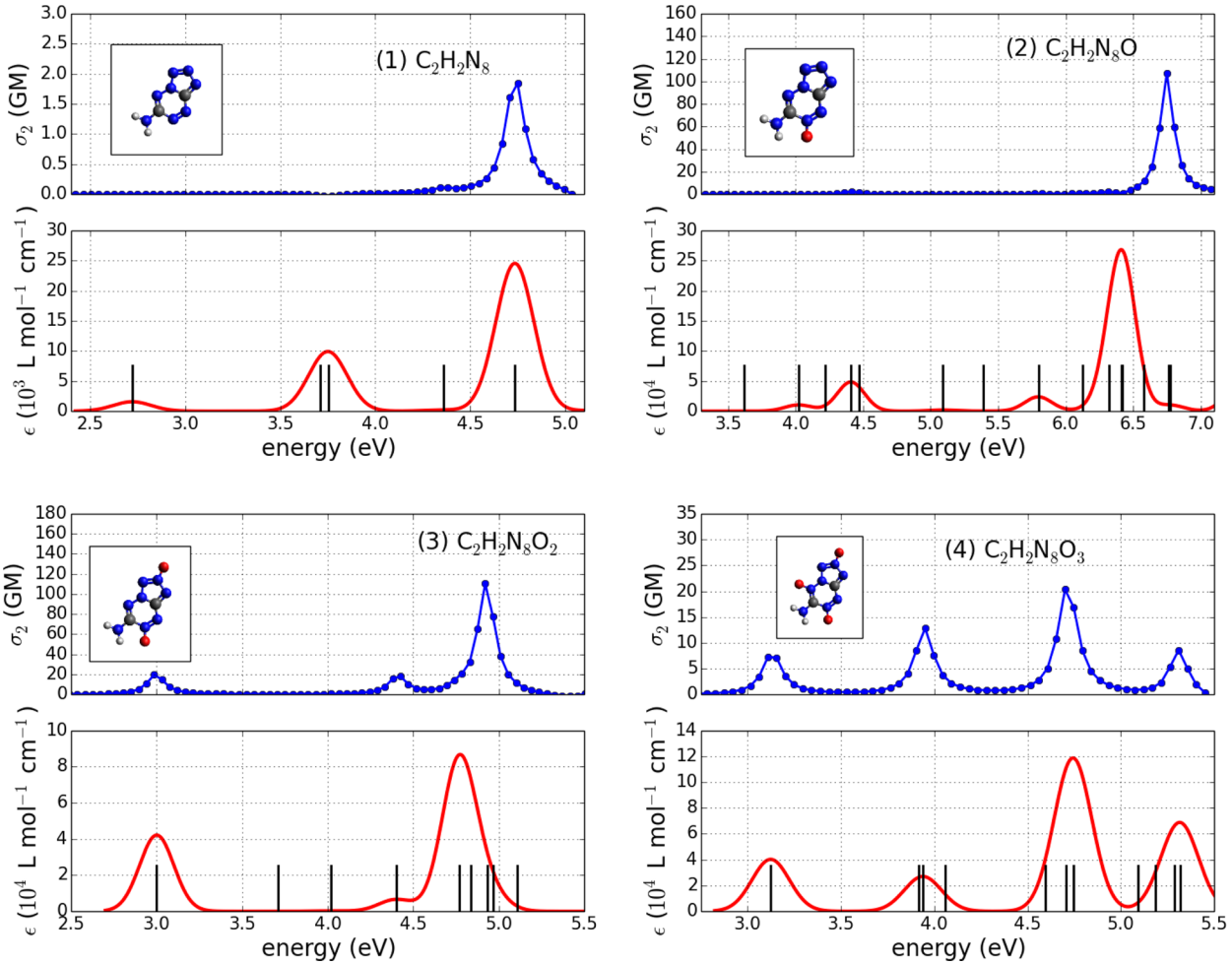

Figure 3. (Bottom) OPA and (top) TPA of molecules **1**–**4** in group I. The energy scale for TPA is given as twice the photon energy required for excitation so that OPA and TPA excitations can be compared.

similar to that in **2**, whereas in **4**, nearly evenly spaced peaks ranging from 7 to 20 GM are present. Molecules **3** and **4** show CT character for TPA-active transitions. For **3**, this involves transfer of electron density from the NH_2 groups to O and from O to the π system; for **4**, the same is observed for the lower two-photon excitations, whereas higher excitations have a more complicated description (Table S1, Supporting Information).

Group II. Group II has two different bicyclic frameworks that vary in terms of the number of N atoms and the placement of a NO_2 substituent. Each framework is further varied by the presence or absence of an O substituent. Optical spectra are given in Figure 4. The simulated OPA spectra show peaks between 4 and 6 eV in the entire series, and in both types of bicyclic frameworks, an additional O substituent adds two significant peaks between 3 and 4 eV. In general, the OPA spectra are similar between the two frameworks.

TPA spectra show significant differences depending on the core type. Molecules **7** and **8** show more intense TPA than **5** and **6**, despite having similar OPA maxima. The two-photon transitions in **5** and **7** have CT character from a NO_2 substituent to the bicyclic framework. Electron transfer from a NH_2 substituent to the bicyclic framework occurs at higher energy. Compared to compound **6**, compound **8** shows an additional peak occurring at ~4.7 eV. Comparing **5** to **6** and **7** to **8**, the presence of an additional O subtituent produces TPA

DOI: 10.1021/acs.jpca.6b03136
J. Phys. Chem. A 2016, 120, 4455–4464

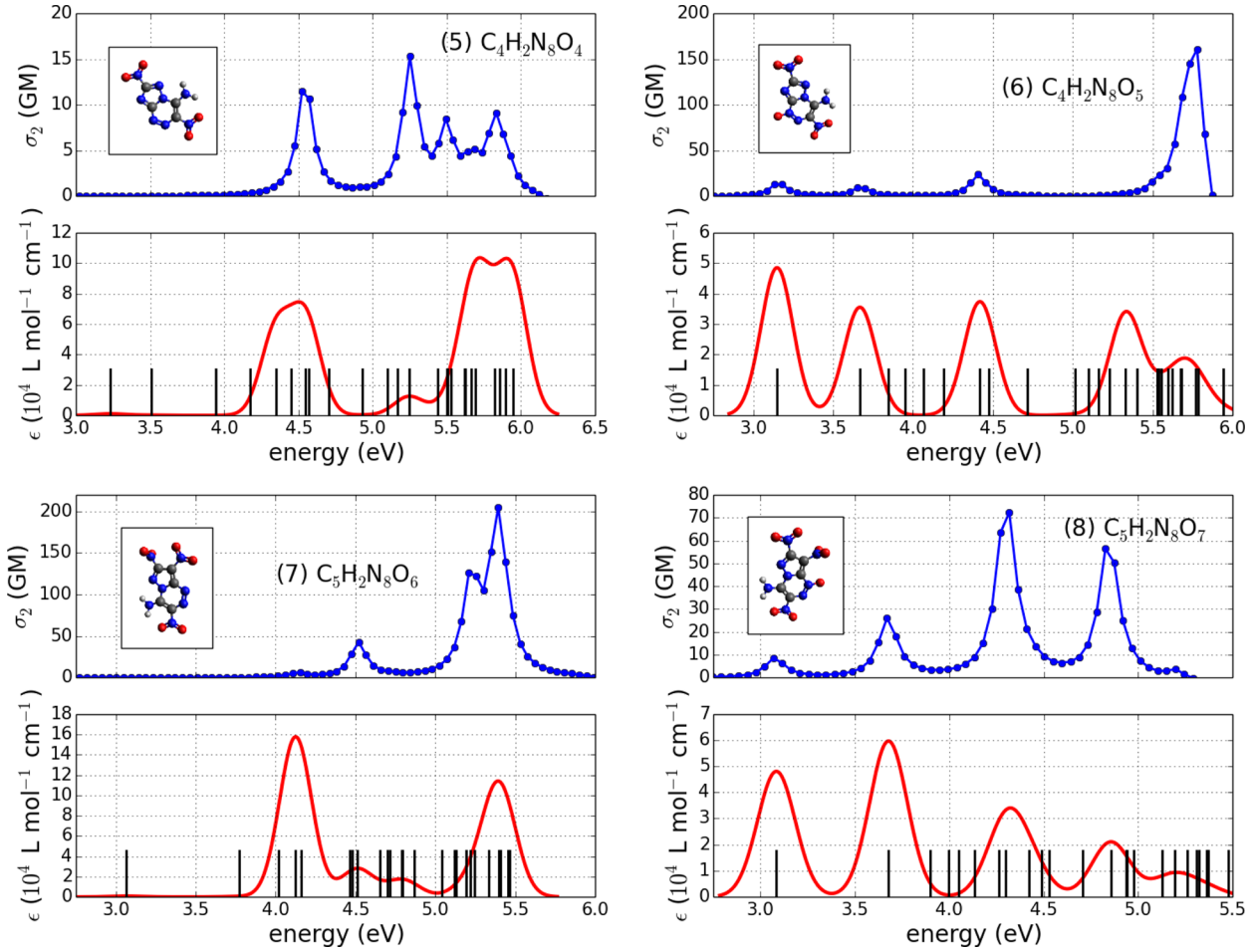

Figure 4. (Bottom) OPA and (top) TPA of molecules **5**–**8** in group II. The energy scale for TPA is given as twice the photon energy required for excitation so that OPA and TPA excitations can be compared.

peaks between 3 and 4 eV and increases the intensity of the peaks between 4 and 5 eV.

Group III. Group III has a tricyclic framework with varying cleavage of the central ring and additional NO_2 substituents. Optical spectra for this group are given in Figure 5. OPA begins at ∼4.2 eV in **9** (uncleaved ring) and ∼5.5 eV in **10** and **11** (cleaved ring). TPA is relatively strong, with maxima at about 40 GM in **9** and 20 GM in **10**. Compared to compound **9**, compound **10** has several transitions that contribute to the main TPA peak. In **11**, NO_2 substituents are attached to the NH moiety (present after ring cleavage). The TPA intensity of the largest peak is reduced compared to those in **9** and **10**. NTO analysis reveals CT from the NO_2 groups to the central ring in **9**. In **10** and **11**, however, CT is from the central ring to the NO_2 groups and from the NO_2 groups to the central ring, respectively, highlighting the effect of adding NO_2 groups to the central backbone.

Group IV. Group IV compounds have a single cyclic system with either two N_3 substituents (**12**), two fluorinated chainlike substituents (**13**), or two fluorinated chainlike substituents and two O substituents (**14**). Optical spectra are given in Figure 6. In **13**, OPA is at 2.2 eV and is the product of a single transition. At ∼4 eV, a second transition occurs. Additional O substituents (**14**) eliminate the low-energy peak, but another appears at 3.4 eV. The simulated TPA of both molecules is low. In **13**, the peak is at ∼3.9 eV at 2 GM, whereas in **14**, several peaks appear between 3.0 and ∼3.36 eV with intensities of about 2.5 GM, respectively. NTO analysis predicts predominant CT from the central ring system to the NO_2 substituents (Table S1, Supporting Information) for these peaks. Upon replacement of the moieties containing NO_2 with N_3 in **12**, the TPA spectral window increases to ∼5.5 eV, and a large TPA response is observed at nearly 300 GM. This response might be present in **13** and **14**, but at energies higher than the allowed spectral window.

DISCUSSION

These simulations predict several two-photon-active transitions for each chromophore considered. Molecules in groups I–III have transitions with intensities above 10 GM, whereas TPA in group IV is relatively weak except for a large transition in molecule **14**. These weak transitions fail to provide active TPA because of the predominant CT character of transitions (Figure S1 in the Supporting Information). A simplified three-level model has been broadly used to describe TPA. It relates TPA intensity to $\mu_{ge}^2\Delta\mu_{ge}^2$, where μ_{ge} is the transition dipole moment between the ground and excited states and $\Delta\mu_{ge}$ is the difference between the ground- and excited-state dipole moments.[12,46] Here, the transition dipole moment will be negligible for predominant CT character; thus, partial CT is essential for strong TPA (according to these simplified models).

In the case of groups I and II, addition of O substituents enhances the optical properties desirably: It increases the TPA

DOI: 10.1021/acs.jpca.6b03136
J. Phys. Chem. A 2016, 120, 4455–4464

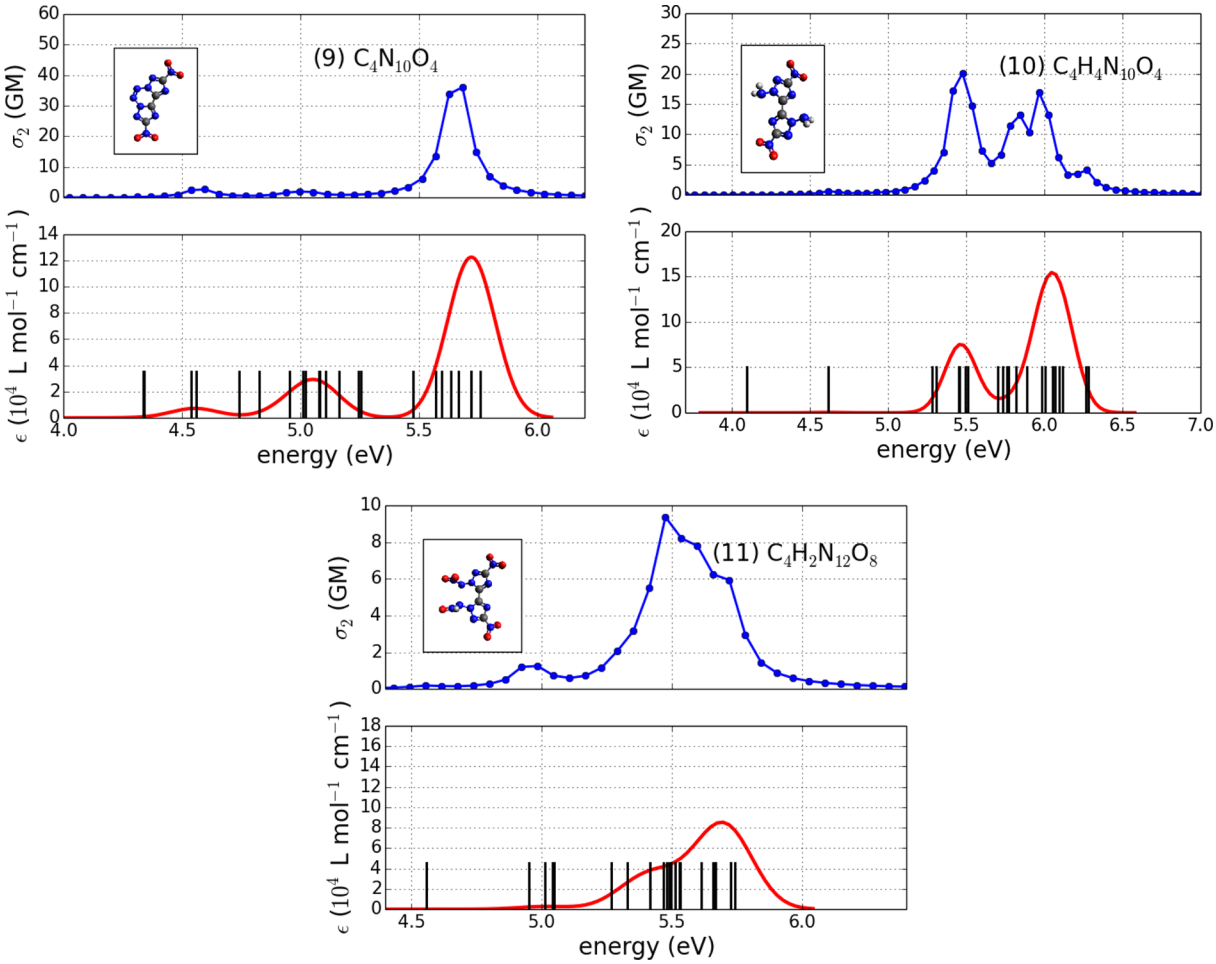

Figure 5. (Bottom) OPA and (top) TPA of molecules **9**−**11** in group III. The energy scale for TPA is given as twice the photon energy required for excitation so that OPA and TPA excitations can be compared.

spectral intensity and lowers the TPA peak energy. It also serves to improve the oxygen balance of these energetic molecules. For the CEMs analyzed here, the OB% value is negative, indicating oxygen deficiency and incomplete oxidation during combustion. In all cases, the OB% value is improved (becoming less negative) with the addition of O substituents. The oxygen balance for each molecule is given in Table 2. This form of chemical substitution seems to have dual benefit for the design of photoactive energetic materials. The systems in group IV are not likely to perform well as two-photon absorbers, and such substitutions do not seem to improve this case. The molecules in group III show relatively strong TPA in the range of ∼6 eV. However, this photon energy is still too high for conventional laser sources.

It might be possible to tune the optical wavelengths and intensities of these molecules using alternative molecular conformations. Optical spectra for local minima of molecules **10**−**14** are given in Figure S1. Molecular conformation is predicted to have an effect on the location and intensity of transitions in molecules **10** and **12**, changing the transition intensities by a factor of 2 and shifting the peaks by up to 0.5 eV. Further studies of these effects will be presented in a future publication.

Optical initiation involves excitation of a material to a dissociative state, thereby igniting an HE. A possible route to selectively excite a two-photon transition uses a frequency-doubled Nd:YAG laser. This requires relatively low two-photon-active energies of about 3.6 eV (twice the energy of a 532-nm photon). Several molecules have transitions near this energy, including **3**, **4**, **6**, and **8**, and therefore show promise for this application.

CONCLUSIONS

The OPA and TPA of novel CEMs were simulated. The theoretical extinction coefficients show strong similarities to experiment for most of the molecules. Significant TPA intensities on the order of 10^2 GM are predicted for several molecules. TPA peaks near ∼3.6 eV with intensities exceeding 10 GM show promise for optical initiation. Calculated optical spectra were compared to experiment and rationalized based on variations in chemical structure.

Several molecules in the series had analogues with additional O substituents. This improves the oxygen balance and increases TPA in molecules of groups I and II. This constitutes an important result that can improve the sensitivity and strength of HEs. Group III was found to have TPA intensities of about 40−50 GM but not within the spectral window of a conventional laser. Molecules in group IV are predicted to have low TPA intensities, which is attributed to predominant CT character of the relevant transitions.

This computational study, supported by experimental data, shows how the optical spectra of CEMs can be controlled by chemical substitution. The identified design principles, found

DOI: 10.1021/acs.jpca.6b03136
J. Phys. Chem. A 2016, 120, 4455−4464

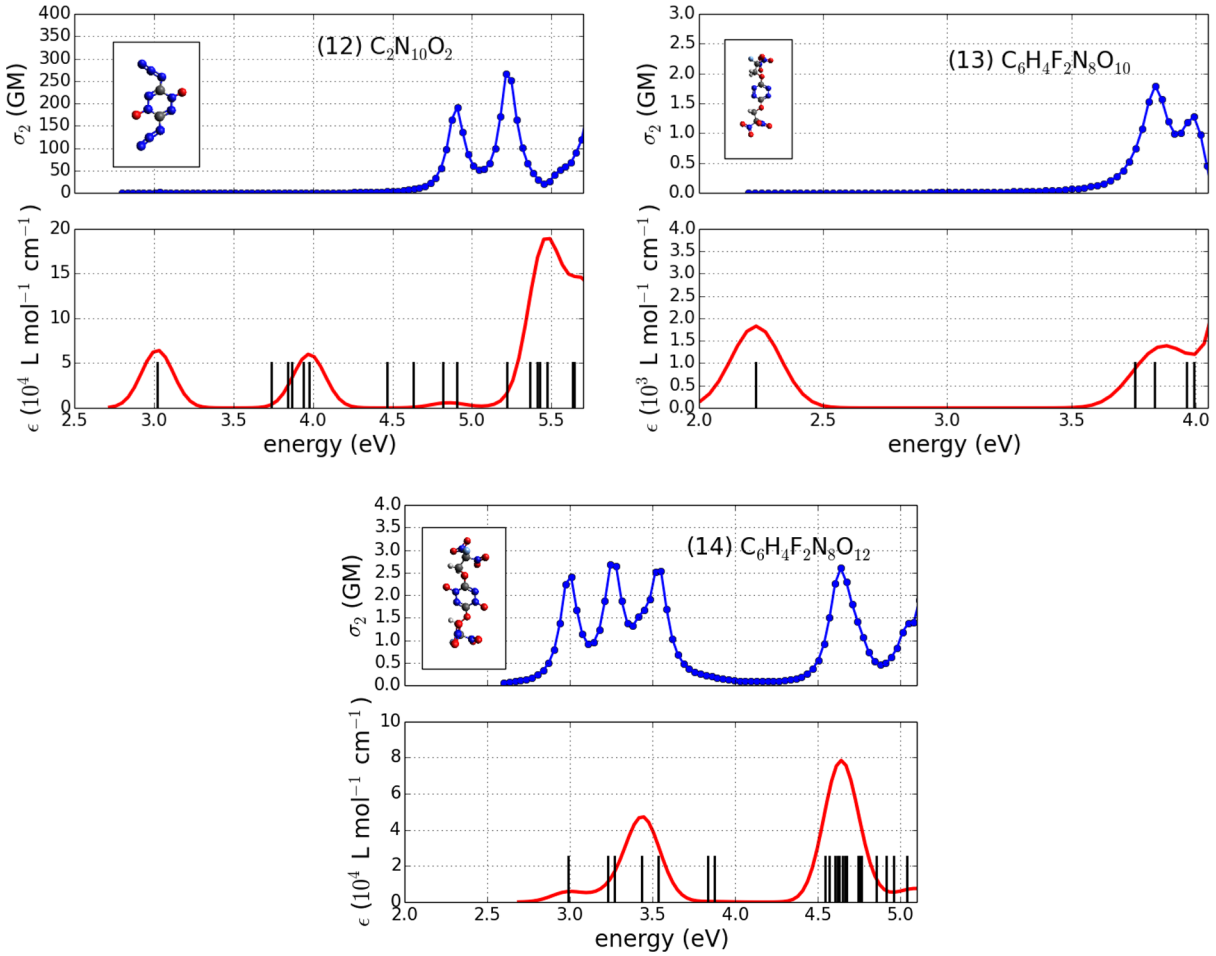

Figure 6. (Bottom) OPA and (top) TPA of molecules **12**−**14** in group IV. The energy scale for TPA is given as twice the photon energy required for excitation so that OPA and TPA excitations can be compared.

Table 2. Numbers of Oxygen Substituents (N_O) and Calculated Oxygen Balances (OB%) for Molecules in Each Grouping

molecule	N_O	OB%
	Group I	
1	0	−57.9
2	1	−41.5
3	2	−28.2
4	3	−17.2
	Group II	
5	0	−35.4
6	1	−26.4
7	0	−29.6
8	1	−22.4
	Group III	
9	0	−182.2
10	0	−37.5
11	0	−4.6
	Group IV	
12	2	−16.6
13	0	−7.6
14	2	16.32

by comparing simulated properties and chemical structures, will be useful for the further design of CEMs. Through future studies of dynamic properties of photoexcited CEMs, design principles that support the branching ratios of photochemical pathways will be examined.

■ ASSOCIATED CONTENT

Supporting Information

The Supporting Information is available free of charge on the ACS Publications website at DOI: 10.1021/acs.jpca.6b03136.

Natural transition orbitals of two-photon-active transitions. One- and two-photon absorption spectra of alternative molecular conformations of molecules **10**−**14** (PDF)

■ AUTHOR INFORMATION

Corresponding Authors

*E-mail: scharff@lanl.gov. Phone: +1-505-667-8351.
*E-mail: serg@lanl.gov. Phone: +1-505-665-5002.

Notes

The authors declare no competing financial interest.

■ ACKNOWLEDGMENTS

The authors acknowledge support of the U.S. Department of Energy through the Los Alamos National Laboratory (LANL) LDRD Program. LANL is operated by Los Alamos National Security, LLC, for the National Nuclear Security Administration of the U.S. Department of Energy under Contract DE-AC52- 06NA25396. This work was done in part at the Center

DOI: 10.1021/acs.jpca.6b03136
J. Phys. Chem. A 2016, 120, 4455−4464

for Nonlinear Studies (CNLS) and the Center for Integrated Nanotechnology (CINT) at LANL. We also acknowledge the LANL Institutional Computing (IC) program for providing computational resources.

REFERENCES

(1) Barzoukas, M.; Blanchard-Desce, M. Molecular Engineering of Push-Pull Dipolar and Quadrupolar Molecules for Two-Photon Absorption: A Multivalence-Bond States Approach. *J. Chem. Phys.* **2000**, *113*, 3951−3959.
(2) Kogej, T.; Beljonne, D.; Meyers, F.; Perry, J. W.; Marder, S. R.; Bredas, J. L. Mechanisms for Enhancement of Two-Photon Absorption in Donor-Acceptor Conjugated Chromophores. *Chem. Phys. Lett.* **1998**, *298*, 1−6.
(3) Masunov, A.; Tretiak, S. Prediction of Two-Photon Absorption Properties for Organic Chromophores Using Time-Dependent Density-Functional Theory. *J. Phys. Chem. B* **2004**, *108*, 899−907.
(4) Badaeva, E. A.; Timofeeva, T. V.; Masunov, A. M.; Tretiak, S. Role of Donor-Acceptor Strengths and Separation on the Two-Photon Absorption Response of Cytotoxic Dyes: a TD-DFT Study. *J. Phys. Chem. A* **2005**, *109*, 7276−7284.
(5) Kauffman, J. F.; Turner, J. M.; Alabugin, I. V.; Breiner, B.; Kovalenko, S. V.; Badaeva, E. A.; Masunov, A.; Tretiak, S. Two-Photon Excitation of Substituted Enediynes. *J. Phys. Chem. A* **2006**, *110*, 241−251.
(6) Drobizhev, M.; Karotki, A.; Kruk, M.; Rebane, A. Resonance Enhancement of Two-Photon Absorption in Porphyrins. *Chem. Phys. Lett.* **2002**, *355*, 175−182.
(7) Drobizhev, M.; Stepanenko, Y.; Dzenis, Y.; Karotki, A.; Rebane, A.; Taylor, P. N.; Anderson, H. L. Extremely Strong Near-IR Two-Photon Absorption in Conjugated Porphyrin Dimers: Quantitative Description with Three-Essential-States Model. *J. Phys. Chem. B* **2005**, *109*, 7223−7236.
(8) Katan, C.; Charlot, M.; Mongin, O.; Le Droumaguet, C.; Jouikov, V.; Terenziani, F.; Badaeva, E.; Tretiak, S.; Blanchard-Desce, M. Simultaneous Control of Emission Localization and Two-Photon Absorption Efficiency in Dissymmetrical Chromophores. *J. Phys. Chem. B* **2010**, *114*, 3152−3169.
(9) Williams-Harry, M.; Bhaskar, A.; Ramakrishna, G.; Goodson, T.; Imamura, M.; Mawatari, A.; Nakao, K.; Enozawa, H.; Nishinaga, T.; Iyoda, M. Giant Thienylene-Acetylene-Ethylene Macrocycles with Large Two-Photon Absorption Cross Section and Semishape-Persistence. *J. Am. Chem. Soc.* **2008**, *130*, 3252−3253.
(10) Clark, A. E. Time-Dependent Density Functional Theory Studies of the Photoswitching of the Two-Photon Absorption Spectra in Stilbene, Metacyclophenadiene, and Diarylethene Chromophores. *J. Phys. Chem. A* **2006**, *110*, 3790−3796.
(11) Terenziani, F.; Morone, M.; Gmouh, S.; Blanchard-Desce, M. Linear and Two-Photon Absorption Properties of Interacting Polar Chromophores: Standard and Unconventional Effects. *ChemPhysChem* **2006**, *7*, 685−696.
(12) Katan, C.; Terenziani, F.; Mongin, O.; Werts, M. H. V.; Porres, L.; Pons, T.; Mertz, J.; Tretiak, S.; Blanchard-Desce, M. Effects of (Multi)branching of Dipolar Chromophores on Photophysical Properties and Two-Photon Absorption. *J. Phys. Chem. A* **2005**, *109*, 3024−3037.
(13) Bartholomew, G. P.; Rumi, M.; Pond, S. J. K.; Perry, J. W.; Tretiak, S.; Bazan, G. C. Two-Photon Absorption in Three-Dimensional Chromophores Based on [2.2]-paracyclophane. *J. Am. Chem. Soc.* **2004**, *126*, 11529−11542.
(14) Badaeva, E.; Tretiak, S. Two Photon Absorption of Extended Substituted Phenylenevinylene Oligomers: a TDDFT Study. *Chem. Phys. Lett.* **2008**, *450*, 322−328.
(15) Drobizhev, M.; Karotki, A.; Dzenis, Y.; Rebane, A.; Suo, Z.; Spangler, C. W. Strong Cooperative Enhancement of Two-Photon Absorption in Dendrimers. *J. Phys. Chem. B* **2003**, *107*, 7540−7543.
(16) Drobizhev, M.; Stepanenko, Y.; Dzenis, Y.; Karotki, A.; Rebane, A.; Taylor, P. N.; Anderson, H. L. Understanding Strong Two-Photon Absorption in π-Conjugated Porphyrin Dimers Via Double-Resonance Enhancement in a Three-Level Model. *J. Am. Chem. Soc.* **2004**, *126*, 15352−15353.
(17) Bhaskar, A.; Ramakrishna, G.; Lu, Z.; Twieg, R.; Hales, J. M.; Hagan, D. J.; Van Stryland, E.; Goodson, T. Investigation of Two-Photon Absorption Properties in Branched Alkene and Alkyne Chromophores. *J. Am. Chem. Soc.* **2006**, *128*, 11840−11849.
(18) Wang, Y.; He, G. S.; Prasad, P. N.; Goodson, T. Ultrafast Dynamics in Multibranched Structures with Enhanced Two-Photon Absorption. *J. Am. Chem. Soc.* **2005**, *127*, 10128−10129.
(19) Drobizhev, M.; Karotki, A.; Rebane, A.; Spangler, C. W. Dendrimer Molecules with Record Large Two-Photon Absorption Cross Section. *Opt. Lett.* **2001**, *26*, 1081−1083.
(20) Varnavski, O.; Yan, X.; Mongin, O.; Blanchard-Desce, M.; Goodson, T. Strongly Interacting Organic Conjugated Dendrimers with Enhanced Two-Photon Absorption. *J. Phys. Chem. C* **2007**, *111*, 149−162.
(21) Bhaskar, A.; Ramakrishna, G.; Lu, Z.; Twieg, R.; Hales, J. M.; Hagan, D. J.; Van Stryland, E.; Goodson, T. Investigation of Two-Photon Absorption Properties in Branched Alkene and Alkyne Chromophores. *J. Am. Chem. Soc.* **2006**, *128*, 11840−11849.
(22) Chavez, D. E.; Hiskey, M. A. 1, 2, 4, 5-tetrazine Based Energetic Materials. *J. Energ. Mater.* **1999**, *17*, 357−377.
(23) Wei, H.; Zhang, J.; Shreeve, J. M. Synthesis, Characterization, and Energetic Properties of 6-amino-tetrazolo[1, 5-b]-1, 2, 4, 5-tetrazine-7-N-oxide: A Nitrogen-Rich Material with High Density. *Chem. - Asian J.* **2015**, *10*, 1130−1132.
(24) Schulze, M. C.; Scott, B. L.; Chavez, D. E. A High Density Pyrazolo-Triazine Explosive (PTX). *J. Mater. Chem. A* **2015**, *3*, 17963−17965.
(25) Chavez, D. E.; Bottaro, J. C.; Petrie, M.; Parrish, D. A. Synthesis and Thermal Behavior of a Fused, Tricyclic 1, 2, 3, 4-Tetrazine Ring System. *Angew. Chem., Int. Ed.* **2015**, *54*, 12973−12975.
(26) Chavez, D. E.; Bottaro, J. C.; Petrie, M.; Parrish, D. A. Synthesis and Thermal Behavior of a Fused, Tricyclic 1, 2, 3, 4-Tetrazine Ring System. *Angew. Chem.* **2015**, *127*, 13165−13167.
(27) Yin, P.; Shreeve, J. M. From N-Nitro to N-Nitroamino: Preparation of High-Performance Energetic Materials by Introducing Nitrogen-Containing Ions. *Angew. Chem., Int. Ed.* **2015**, *54*, 14513−14517.
(28) Cooper, P. W. *Explosives Engineering*; Wiley: New York, 1996.
(29) Greenfield, M. T.; McGrane, S. D.; Bolme, C. A.; Bjorgaard, J. A.; Nelson, T. R.; Tretiak, S.; Scharff, R. J. Photoactive High Explosives: Linear and Nonlinear Photochemistry of Petrin Tetrazine Chloride. *J. Phys. Chem. A* **2015**, *119*, 4846−4855.
(30) Bykhalo, A. I.; Zhuzhukalo, E. V.; Koval'skii, N. G.; Kolomiiskii, A. N.; Korobov, V. V.; Rozhkov, A. D.; Yudin, A. I. Initiation of PETN by High-Power Laser Radiation. *Combust., Explos. Shock Waves* **1985**, *21*, 481−483.
(31) Tarzhanov, V. I.; Zinchenko, A. D.; Sdobnov, V. I.; Tokarev, B. B.; Pogrebov, A. I.; Volkova, A. A. Laser Initiation of PETN. *Combust., Explos. Shock Waves* **1996**, *32*, 454−459.
(32) Aluker, E. D.; Krechetov, A. G.; Mitrofanov, A. Y.; Nurmukhametov, D. R. Photochemical and Photothermal Dissociation of PETN During Laser Initiation. *Russ. J. Phys. Chem. B* **2011**, *5*, 658−660.
(33) Nelson, T. R.; Bjorgaard, J. A.; Greenfield, M. T.; Bolme, C. A.; Brown, K. E.; McGrane, S. D.; Scharff, R. J.; Tretiak, S. Ultrafast Photodissociation Dynamics of Nitromethane. *J. Phys. Chem. A* **2016**, *120*, 519−526.
(34) Casida, M. E. Time-Dependent Density Functional Response Theory for Molecules. In *Recent Advances in Density-Functional Methods*, Part I; Chong, D. P., Ed.; World Scientific: Singapore, 1995; Vol. *1*, p 155.
(35) Tretiak, S.; Chernyak, V. Resonant Nonlinear Polarizabilities in the Time-Dependent Density Functional (TDDFT) Theory. *J. Chem. Phys.* **2003**, *119*, 8809−8823.

DOI: 10.1021/acs.jpca.6b03136
J. Phys. Chem. A 2016, 120, 4455−4464

(36) Jacquemin, D.; Wathelet, V.; Perpete, E. A.; Adamo, C. Extensive TD-DFT Benchmark: Singlet-Excited States of Organic Molecules. *J. Chem. Theory Comput.* **2009**, *5*, 2420−2435.
(37) Dreuw, A.; Head-Gordon, M. Single-Reference Ab Initio Methods for the Calculation of Excited States of Large Molecules. *Chem. Rev.* **2005**, *105*, 4009−4037.
(38) Szabo, A.; Ostlund, N. S. *Modern Quantum Chemistry: Introduction to Advanced Electronic Structure Theory*, revised ed.; McGraw-Hill: New York, 1996.
(39) Becke, A. D. Density-Functional Thermochemistry. 3. The Role of Exact Exchange. *J. Chem. Phys.* **1993**, *98*, 5648−5652.
(40) Terenziani, F.; Katan, C.; Badaeva, E.; Tretiak, S.; Blanchard-Desce, M. Enhanced Two-Photon Absorption of Organic Chromophores: Theoretical and Experimental Assessments. *Adv. Mater.* **2008**, *20*, 4641−4678.
(41) Frisch, M. J.; Trucks, G. W.; Schlegel, H. B.; Scuseria, G. E.; Robb, M. A.; Cheeseman, J. R.; Montgomery, J. A., Jr.; Vreven, T.; Kudin, K. N.; Burant, J. C.; Millam, J. M.; Iyengar, S. S.; Tomasi, J.; Barone, V.; Mennucci, B.; Cossi, M.; Scalmani, G.; Rega, N.; Petersson, G. A.; Nakatsuji, H.; Hada, M.; Ehara, M.; Toyota, K.; Fukuda, R.; Hasegawa, J.; Ishida, M.; Nakajima, T.; Honda, Y.; Kitao, O.; Nakai, H.; Klene, M.; Li, X.; Knox, J. E.; Hratchian, H. P.; Cross, J. B.; Bakken, V.; Adamo, C.; Jaramillo, J.; Gomperts, R.; Stratmann, R. E.; Yazyev, O.; Austin, A. J.; Cammi, R.; Pomelli, C.; Ochterski, J. W.; Ayala, P. Y.; Morokuma, K.; Voth, G. A.; Salvador, P.; Dannenberg, J. J.; Zakrzewski, V. G.; Dapprich, S.; Daniels, A. D.; Strain, M. C.; Farkas, O.; Malick, D. K.; Rabuck, A. D.; Raghavachari, K.; Foresman, J. B.; Ortiz, J. V.; Cui, Q.; Baboul, A. G.; Clifford, S.; Cioslowski, J.; Stefanov, B. B.; Liu, G.; Liashenko, A.; Piskorz, P.; Komaromi, I.; Martin, R. L.; Fox, D. J.; Keith, T.; Al-Laham, M. A.; Peng, C. Y.; Nanayakkara, A.; Challacombe, M.; Gill, P. M. W.; Johnson, B.; Chen, W.; Wong, M. W.; Gonzalez, C.; Pople, J. A. *Gaussian 03*, revision E.01; Gaussian, Inc.: Wallingford, CT, 2004.
(42) Frisch, M. J.; Trucks, G. W.; Schlegel, H. B.; Scuseria, G. E.; Robb, M. A.; Cheeseman, J. R.; Scalmani, G.; Barone, V.; Mennucci, B.; Petersson, G. A.; Nakatsuji, H.; Caricato, M.; Li, X.; Hratchian, H. P.; Izmaylov, A. F.; Bloino, J.; Zheng, G.; Sonnenberg, J. L.; Hada, M.; Ehara, M.; Toyota, K.; Fukuda, R.; Hasegawa, J.; Ishida, M.; Nakajima, T.; Honda, Y.; Kitao, O.; Nakai, H.; Vreven, T.; Montgomery, J. A., Jr.; Peralta, J. E.; Ogliaro, F.; Bearpark, M.; Heyd, J. J.; Brothers, E.; Kudin, K. N.; Staroverov, V. N.; Keith, T.; Kobayashi, R.; Normand, J.; Raghavachari, K.; Rendell, A.; Burant, J. C.; Iyengar, S. S.; Tomasi, J.; Cossi, M.; Rega, N.; Millam, J. M.; Klene, M.; Knox, J. E.; Cross, J. B.; Bakken, V.; Adamo, C.; Jaramillo, J.; Gomperts, R.; Stratmann, R. E.; Yazyev, O.; Austin, A. J.; Cammi, R.; Pomelli, C.; Ochterski, J. W.; Martin, R. L.; Morokuma, K.; Zakrzewski, V. G.; Voth, G. A.; Salvador, P.; Dannenberg, J. J.; Dapprich, S.; Daniels, A. D.; Farkas, Ö.; Foresman, J. B.; Ortiz, J. V.; Cioslowski, J.; Fox, D. J. *Gaussian 09*, revision D.01; Gaussian, Inc., Wallingford, CT, 2009.
(43) Martin, R. L. Natural transition orbitals. *J. Chem. Phys.* **2003**, *118*, 4775−4777.
(44) Hanwell, M. D.; Curtis, D. E.; Lonie, D. C.; Vandermeersch, T.; Zurek, E.; Hutchison, G. R. Avogadro: An Advanced Semantic Chemical Editor, Visualization, and Analysis Platform. *J. Cheminf.* **2012**, *4*, 17.
(45) Bjorgaard, J. A.; Nelson, T.; Kalinin, K.; Kuzmenko, V.; Velizhanin, K. A.; Tretiak, S. Simulations of Fluorescence Solvatochromism in Substituted PPV Oligomers from Excited State Molecular Dynamics with Implicit Solvent. *Chem. Phys. Lett.* **2015**, *631*−*632*, 66−69.
(46) Hales, J. M.; Hagan, D. J.; Van Stryland, E. W.; Schafer, K. J.; Morales, A. R.; Belfield, K. D.; Pacher, P.; Kwon, O.; Zojer, E.; Bredas, J. L. Resonant Enhancement of Two-Photon Absorption in Substituted Fluorene Molecules. *J. Chem. Phys.* **2004**, *121*, 3152−3160.

DOI: 10.1021/acs.jpca.6b03136
J. Phys. Chem. A 2016, 120, 4455−4464